

# Experimental setups for FEL-based four-wave mixing experiments at FERMI

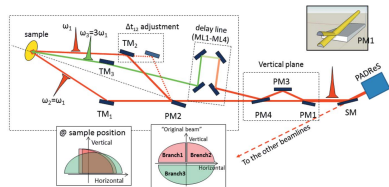
Filippo Bencivenga,<sup>a,\*</sup> Marco Zangrando,<sup>a,b</sup> Cristian Svetina,<sup>a,c</sup> Alessandro Abrami,<sup>a</sup> Andrea Battistoni,<sup>d</sup> Roberto Borghes,<sup>a</sup> Flavio Capotondi,<sup>a</sup> Riccardo Cucini,<sup>a</sup> Francesco Dallari,<sup>e</sup> Miltcho Danailov,<sup>a</sup> Alexander Demidovich,<sup>a</sup> Claudio Fava,<sup>a</sup> Giulio Gaio,<sup>a</sup> Simone Gerusina,<sup>a</sup> Alessandro Gessini,<sup>a</sup> Fabio Giacuzzo,<sup>a</sup> Riccardo Gobessi,<sup>a</sup> Roberto Godnig,<sup>a</sup> Riccardo Grisonich,<sup>a</sup> Maya Kiskinova,<sup>a</sup> Gabor Kurdi,<sup>a</sup> Giorgio Loda,<sup>a</sup> Marco Lonza,<sup>a</sup> Nicola Mahne,<sup>a</sup> Michele Manfredda,<sup>a</sup> Riccardo Mincigrucci,<sup>a,f</sup> Gianpiero Pagon,<sup>a</sup> Pietro Parisse,<sup>a</sup> Roberto Passuello,<sup>a</sup> Emanuele Pedersoli,<sup>a</sup> Lorenzo Pivetta,<sup>a</sup> Milan Prica,<sup>a</sup> Emiliano Principi,<sup>a</sup> Iliaria Rago,<sup>a,c</sup> Lorenzo Raimondi,<sup>a</sup> Roberto Sauro,<sup>a</sup> Martin Scarcia,<sup>a</sup> Paolo Sigalotti,<sup>a</sup> Maurizio Zaccaria<sup>a</sup> and Claudio Masciovecchio<sup>a</sup>

<sup>a</sup>ELETTRA-Sincrotrone Trieste SCpA, SS 14, km 163.5 in AREA Science Park, Basovizza, 34149 Trieste, Italy, <sup>b</sup>IOM-CNR, Laboratorio TASC, SS 14, km 163.5 in AREA Science Park, Basovizza, 34149 Trieste, Italy, <sup>c</sup>Graduate School of Nanotechnology, University of Trieste, Piazzale Europa 1, 34127 Trieste, Italy, <sup>d</sup>PULSE Institute for Ultrafast Energy Science, SLAC, Stanford University, Menlo Park, Stanford, CA 94305, USA, <sup>e</sup>Physics Department, University of Trento, Trento, Italy, and <sup>f</sup>Department of Physics and Geology, University of Perugia, Perugia, Italy. \*Correspondence e-mail: filippo.bencivenga@elettra.eu

The recent advent of free-electron laser (FEL) sources is driving the scientific community to extend table-top laser research to shorter wavelengths adding elemental selectivity and chemical state specificity. Both a compact setup (mini-TIMER) and a separate instrument (EIS-TIMER) dedicated to four-wave-mixing (FWM) experiments has been designed and constructed, to be operated as a branch of the Elastic and Inelastic Scattering beamline: EIS. The FWM experiments that are planned at EIS-TIMER are based on the transient grating approach, where two crossed FEL pulses create a controlled modulation of the sample excitations while a third time-delayed pulse is used to monitor the dynamics of the excited state. This manuscript describes such experimental facilities, showing the preliminary results of the commissioning of the EIS-TIMER beamline, and discusses original experimental strategies being developed to study the dynamics of matter at the fs–nm time–length scales. In the near future such experimental tools will allow more sophisticated FEL-based FWM applications, that also include the use of multiple and multi-color FEL pulses.

## 1. Introduction

The unique properties of optical lasers, in particular the high brightness and coherence, have permitted the development of non-linear optics (Bloembergen, 1982). To date, applications based on the non-linear optical approach are widespread in all fields of physics, chemistry and biology, and are used to probe the more disparate kind of dynamics and fundamental processes. The multi-wave nature of these methods, the possibility to combine ultrafast time resolution with energy and wavevector selectivity, as well as the capability to probe processes inaccessible by linear methods, resulted in a large number of cutting-edge applications, ranging from, for example, sub-wavelength imaging (Lewis & Lieberman, 1991) to quantum communications (Li *et al.*, 2005). The availability of bright and coherent ultrafast extreme-ultraviolet (EUV)



and X-ray sources, such as free-electron lasers (FELs), have allowed the first pioneering experiments on non-linear optics in the EUV/X-ray range. The extension of non-linear optical methods at sub-optical wavelengths, in particular those based on third-order processes, also referred to as four-wave mixing (FWM), has been conceived more than a decade ago (Tanaka & Mukamel, 2002). Theoretically it has been shown how EUV/soft X-ray FWM can enable elemental selectivity and the study of dynamics of high-energy electron excitations such as, for example, valence band excitons. This provides a unique possibility to detect in real time and on nanometer length scale ultrafast vibrational dynamics, structural relaxations and elementary excitations (phonons, polarons *etc.*), as well as charge and energy flows among different atoms in a sample, in addition to the capability to probe the correlations among such different dynamical processes. Furthermore, dipole-forbidden optical transitions can be observed at X-ray wavelengths, hence enabling the detection of the entire excitation spectrum.

On the experimental side, the development of EUV and X-ray FELs in the last few years has permitted observation of the occurrence of coherent non-linear processes, such as stimulated emission (Rohringer *et al.*, 2012), amplified spontaneous emission (Beye *et al.*, 2013), two-photon absorption (Tamasaku *et al.*, 2014) and second-order wave-mixing (Glover *et al.*, 2012; Shwartz *et al.*, 2014); still without the determination of the time dependence of such non-linear signals. The fully coherent EUV pulses of the FERMI seeded FEL [Elettra, Trieste, Italy (Allaria *et al.*, 2012a)], in combination with a specially designed experimental setup (mini-TIMER), have been used to demonstrate a FEL-stimulated third-order non-linear response (Bencivenga *et al.*, 2015a) and to detect its time dependence in an extended range (*i.e.* up to 100 ps). The latter is compatible with a time-dependent impulsive stimulated scattering signal, a specific type of FWM experiment routinely used in the optical domain to probe vibrational dynamics (Dhar *et al.*, 1994). Most recently (July 2015) we started the commissioning of another experimental facility for EUV/soft X-ray FWM, EIS-TIMER, which shares with mini-TIMER the basic experimental geometry, but will permit a much larger wavevector ( $k$ ) range to be probed, up to the inverse nanometer range. The wavevector range between 0.1 and 1 nm<sup>-1</sup> is actually of the greatest relevance for the study of dynamics in nanostructures, crystals featured by incommensurate lattice vectors and systems without translational invariance (*e.g.* glasses and liquids). The latter are characterized by marked anomalies with respect to the crystalline counterparts, whose understanding is motivating strong experimental and theoretical efforts. Despite that, different and discordant theories can still explain equally well the experimental data and unambiguously indicate that the key role in solving the puzzle can be found in the study of the collective vibrational dynamics in the 0.1–1 nm<sup>-1</sup>  $k$ -range. Nowadays, this range is not fully accessible by the methods commonly used to probe vibrational dynamics, even though the recent efforts in the development of broadband pico-acoustics (Ferrante *et al.*, 2013) and sub-meV inelastic hard

X-ray scattering (Shvyd'ko *et al.*, 2014) are going to quickly change this situation.

We hereby report on the main features and complementarities between the setups we developed for FEL-based FWM experiments, on the first results achieved by using these unique instruments and on their possible applications.

## 2. Experimental facilities for FEL-based FWM at FERMI

Our project to build up a FEL-based FWM instrument (EIS-TIMER) dates back to 2008 and was initially focused on the study of vibrational dynamics in condensed matter, in particular on disordered systems and nanostructures, in the (nm<sup>-1</sup>, THz)-range (Bencivenga & Masciovecchio, 2009). The natural choice for this kind of applications is impulsive stimulated scattering (ISS), which in the optical domain is usually achieved through the so-called transient grating (TG) approach (Nelson *et al.*, 1982; Dhar *et al.*, 1994).

In a FWM experiment (see Fig. 1a) three coherent beams of frequency/wavevector/polarization  $\omega_i/k_i/n_i$  ( $i = 1, 2, 3$ ) are brought into interaction in a sample (Bloembergen, 1982; Boyd, 2008). These three light fields are coupled into the sample through a rank-4 tensor, usually referred to as third-order non-linear susceptibility [ $\chi^{(3)}$ ]. Such interactions may result into a non-linear signal that has the form of a well defined ‘macroscopic’ beam propagating downstream from the sample. The photon frequency and wavevector of this fourth beam is a combination of those of the input fields, a condition usually referred to as ‘phase matching’, which is a consequence of the energy–momentum conservation laws and of the coherent nature of wave-mixing processes. Along the direction defined by the phase-matched wavevector the amplitudes of the non-linear fields radiated at the phase-matched frequency by different portions of the sample (located within the coherence length of the process) add coherently, thus resulting in a substantial increase of the non-linear signal that, in some cases, can be as intense as the input beams. Furthermore, since the FWM signal can have a given photon frequency and momentum, not necessarily equal to any frequency–momentum of the input beams, both spatial and spectral discrimination is possible, hence leading to a remarkable increase in the signal-to-noise ratio. Depending on the combination of the input field parameters (photon frequency, momentum, polarization, arrival time, bandwidth, *etc.*) and those of the output field, different kinds of FWM processes can be observed, many of them associated with different and often complementary information. The FWM signal is hence reordered as a function of these parameters (or a combination of them). For instance, in Figs. 1(a) and 1(b) we report the case where two input fields at frequency  $\omega_1$  and  $\omega_2$  are used to stimulate a low-energy excitation (*e.g.* a vibrational mode) of frequency  $\omega_{\text{ex}} = \omega_1 - \omega_2$ , while the third beam ( $\omega_3$ ) probes such an excitation by stimulating the emission of a signal beam at  $\omega_4 = \omega_1 - \omega_2 + \omega_3$  and  $k_4 = k_1 - k_2 + k_3$ . The FWM signal as a function of  $\omega_1 - \omega_2$  (coherent Raman scattering) then contains information on the excitation spectrum, that at fixed  $\omega_1 - \omega_2$  as a function of time delay ( $\Delta t_{23}$ ) between

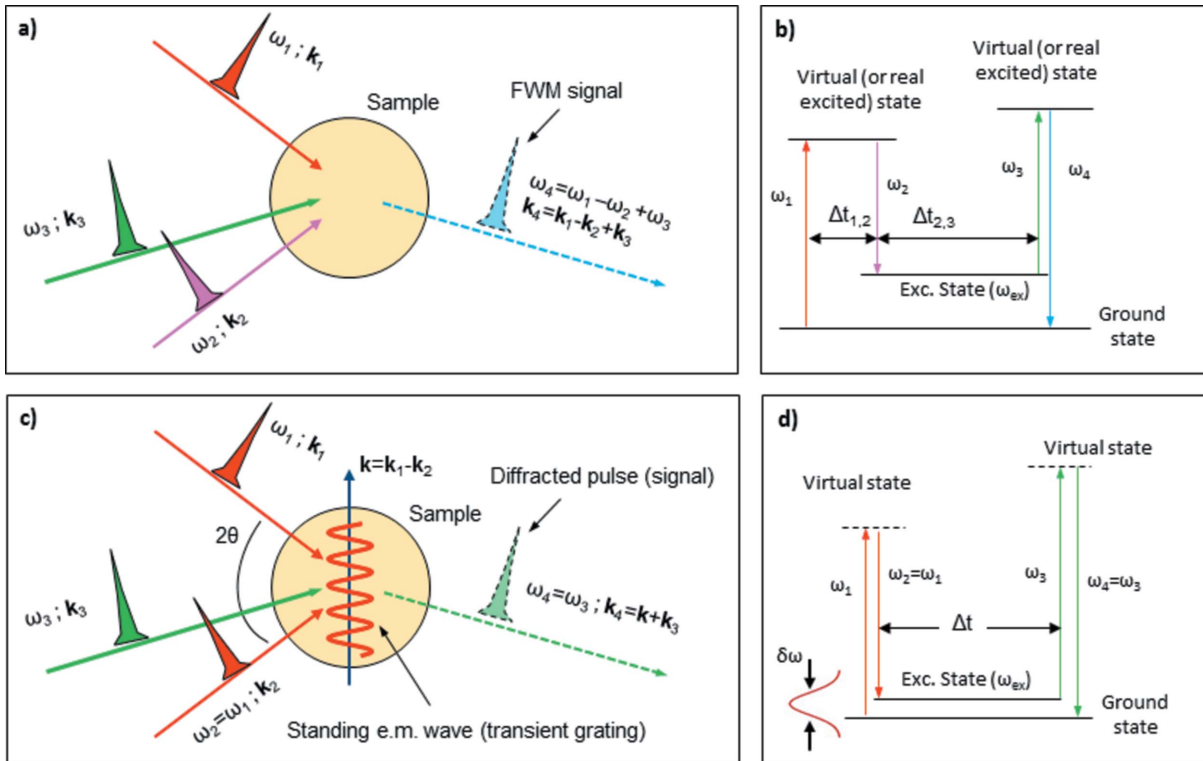


Figure 1 Sketch (a) and energy level scheme (b) for a generic FWM experiment; panels (c) and (d) are as (a) and (b), respectively, for an ISS experiment based on the transient grating approach.

the creation and probing processes carry out information on the time evolution of the selected excitation, while the dependence on  $\Delta t_{12}$  can be related to correlations between the low- and high-energy excited states. Such a large number of possible interactions makes FWM an extremely informative and versatile experimental tool, as widely demonstrated by the wealth of methods and results obtained in the optical domain.

Figs. 1(c) and 1(d) show a typical ISS experiment based on TG, where  $\omega_1 = \omega_2$  and  $\Delta t_{12} = 0$ . In this situation the sample excitations that can be created and probed are those having wavevector equal to that of the induced TG (i.e.  $k_{ex} = k_1 - k_2$ ) and characteristic frequencies within the bandwidth of the excitation pulses ( $\delta\omega$ ) or, in other words, those being slower than the time duration of the photon pulse. Besides this constraint in the spectral range of accessible excitations, ISS is a very general process that can be applied on any dynamical variable coupled to the light field, even those uncoupled in the linear approximation [such as, for example, spin waves (Cameron *et al.*, 1996)].

Besides the fundamental problem related to the fast drop in the  $\chi^{(3)}$ -values as a function of the photon frequency (Patterson, 2010; Bencivenga *et al.*, 2013), severe practical difficulties have hampered the development of the FWM approach in the EUV/X-ray range. One of the main issues is the low brightness of fully coherent sources (such as high-harmonic-generation lasers) and the low longitudinal coherence of the brighter ones (such as FEL devices based on the

self-amplified spontaneous emission process). In this respect seeded FELs, such as FERMI, represent the best trade-off, as they can ensure almost fully coherent photon pulses with sufficient brightness. In addition, issues related to the handling of multiple (and possibly multi-color) FEL pulses are clearly relevant. In this manuscript we present the devices we developed to cope with these issues.

### 2.1. mini-TIMER

In order to demonstrate the feasibility of FEL-based FWM and to anticipate some of the issues that we expect from the commissioning of EIS-TIMER, we devised a compact (580 mm  $\times$  280 mm, excluding the detector) experimental setup (mini-TIMER; see Fig. 2) to be used both as a test facility for the EIS-TIMER instrument and for user experiments. Indeed, as pointed out further below, mini-TIMER has some complementary features with respect to EIS-TIMER, which may be profitably exploited for FWM applications different from ISS. This setup is based on three small (70 mm long and 30 mm high) carbon-coated plane mirrors. One of the three mirrors (M1) works as a wavefront beamsplitter to divide the incoming FEL beam into two halves, a solution already implemented in our laser laboratory in a test setup for optical TG (Cucini *et al.*, 2011a, 2014) that also permits the wavelength and polarization tunability offered by the FERMI FEL to be exploited (Allaria *et al.*, 2012b, 2014). The other two mirrors (M2 and M3) are used to cross the two FEL half-

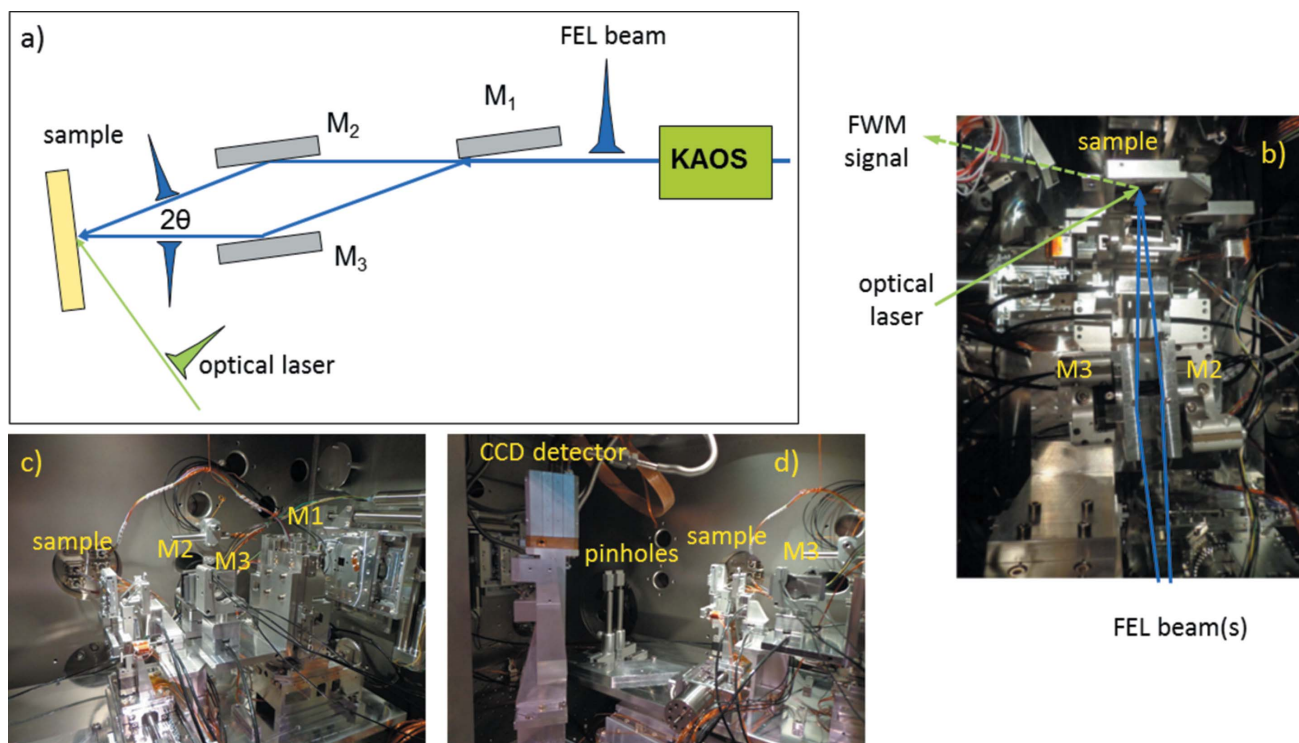
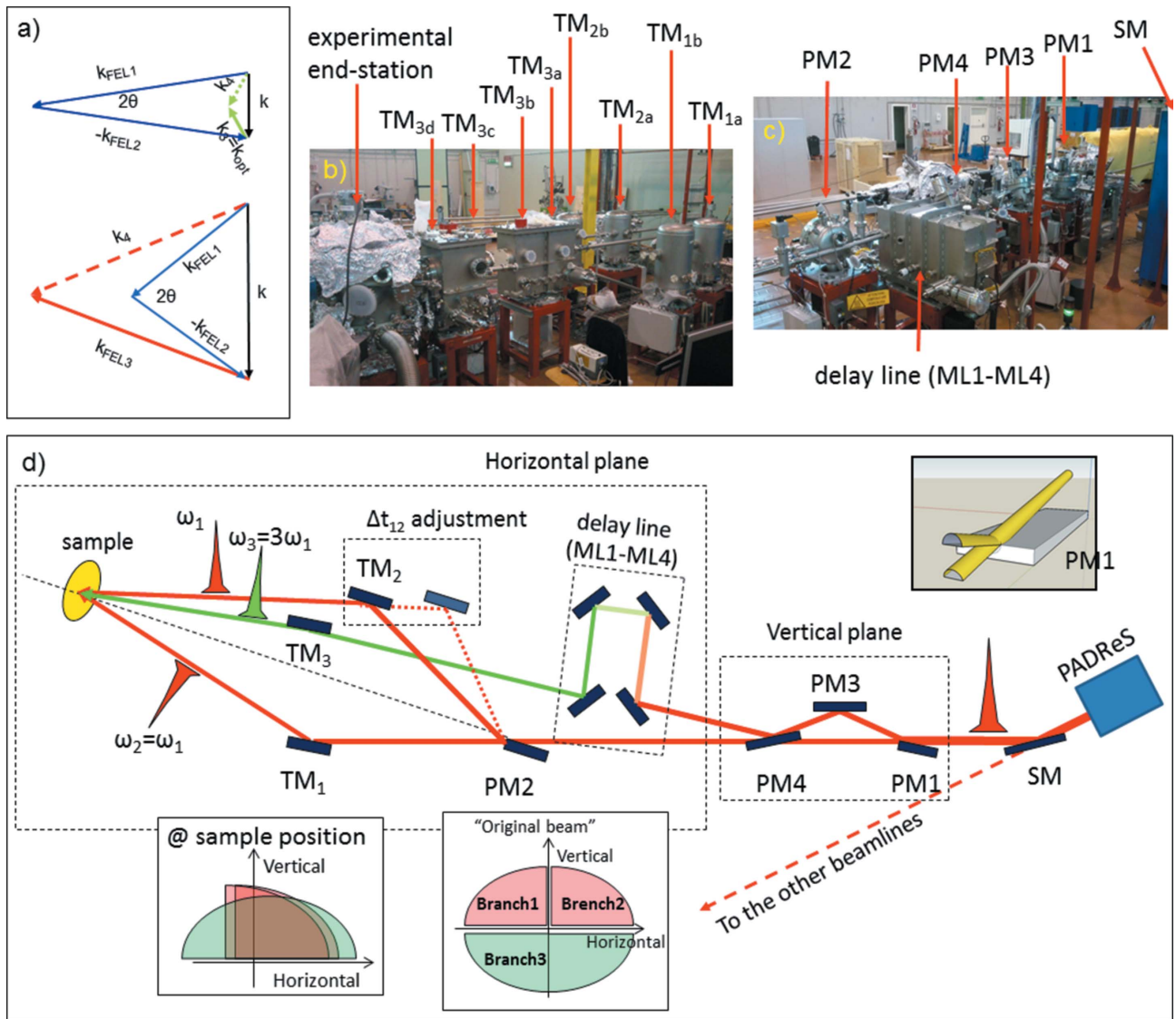


Figure 2  
Sketch (a) and photographs (b, c and d) of the mini-TIMER setup.

beams at the sample with a given crossing angle (the design value is  $2\theta = 6^\circ$ ; the  $\sim 2\text{--}15^\circ$  range is in principle possible) and in time-coincident conditions (variable time delays within the  $\sim 1$  ps range are in principle possible). Time coincidence can be verified on-line using an integrated system for cross-correlation measurements, based on the determination of FEL-induced ultrafast optical reflectivity changes; with respect to our first experiment we improved the accuracy of such a tool (Bencivenga *et al.*, unpublished). More details on the setup and on our first experiment can be found elsewhere (Bencivenga *et al.*, 2015a,b). The mini-TIMER system does not have its own focusing optics, so that it requires an external focusing device. In particular, it is designed to be hosted by the DiProI experimental end-station (Capotondi *et al.*, 2013, 2015), equipped with a Kirkpatrick–Baez active optical system [KAOS (Raimondi *et al.*, 2013; Zangrando *et al.*, 2015)], but it can in principle be hosted by other experimental end-stations. The main limitation of this setup is the impossibility to generate and handle a third FEL beam (*i.e.* to apply a variable time delay and send it into the sample along the required phase-matching direction), which is needed for all FEL-based FWM experiments. FWM applications at mini-TIMER hence rely upon the use of an additional optical pulse. This limits the  $k$ -values at which the phase matching can be achieved to twice the optical wavevector (see Fig. 3a), *i.e.*  $\sim 0.04\text{--}0.06\text{ nm}^{-1}$  by using UV pulses (*e.g.* the third or fourth harmonic of a Ti:sapphire laser). Such a limitation is removed by using a third EUV/soft X-ray pulse, *e.g.* by using a high-harmonic-generation source or a third FEL beam. The latter solution is the one that will be implemented at EIS-TIMER.

## 2.2. EIS-TIMER

The main task of EIS-TIMER is to realise FWM experiments, in particular those based on ISS processes and on the TG geometry, using three FEL beams (Bencivenga & Masciovecchio, 2009; Cucini *et al.*, 2011b; Masciovecchio *et al.*, 2015). This will allow the limitation on the maximum value of the  $k$ -vector in FEL-based FWM experiments involving optical pulses to be overcome (see Fig. 3a). Some photographs of the EIS-TIMER system are displayed in Figs. 3(b)–3(c), while a schematic drawing of the optical layout is reported in Fig. 3(d). The FEL beam exiting from the photon analysis, delivery and reduction system [PADReS (Zangrando *et al.*, 2009, 2015), not shown in Fig. 3(d)] is first split into two halves by a wavefront-division plane mirror [PM1,  $2^\circ$  grazing incidence,  $260\text{ mm} \times 60\text{ mm} \times 50\text{ mm}$  (length  $\times$  width  $\times$  thickness), Au-coated] working in the vertical plane. The beam deflected upwards by PM1 is brought back into the horizontal plane by two other plane mirrors (PM3 and PM4,  $4^\circ$  and  $2^\circ$  grazing incidence,  $140\text{ mm} \times 60\text{ mm} \times 50\text{ mm}$  and  $260\text{ mm} \times 30\text{ mm} \times 50\text{ mm}$ , respectively, Au-coated) with a lateral offset of about 20 mm with respect to the half-beam that freely propagates after PM1. At this stage of the photon transport system we have two almost parallel FEL beams in the horizontal plane with similar transverse profiles. The half-beam that goes through the PM1–PM3–PM4 sequence is routed through a 680 mm-long delay line made out of four multilayer mirrors (ML, angle of incidence  $45^\circ$ , 25.4 mm diameter, 6 mm thickness) while the second half-beam is further split into two halves by a second wavefront-division plane mirror (PM2,  $5^\circ$



**Figure 3** (a) Phase-matching diagram for a FWM experiment involving two EUV/soft X-ray pulses and an optical pulse (top) and that involving three EUV/soft X-ray pulses (bottom); the black arrow is the  $k$ -vector. Photographs (b and c) of the EIS-TIMER photon transport system; the chambers hosting the  $TM_{1c,1d}$  and  $TM_{2c,2d}$  mirrors are not installed, SM is an upstream plane switching mirror (not shown). A sketch of the photon transport system is displayed in (d); sketches of the transverse profiles of the FEL beams along the photon transport systems are shown in the insets.

grazing incidence, 210 mm × 60 mm × 50 mm, Au-coated) working in the horizontal plane. Finally, the three beams are focused at the sample position by a set of three toroidal mirrors (TM, grazing incidence in the 2.2–28.8° range,  $L \times 40 \text{ mm} \times 40 \text{ mm}$ , with  $L$  in the 80–310 mm range, Au-, C- or Ni-coated, depending on the configuration), which are placed in such a way that phase matching is achieved for photon frequencies  $\omega_1 = \omega_2$  and  $\omega_3 = 3\omega_1$ ; here the indices 1 and 2 indicate the two external branch-lines while the index 3 is for the internal one, the latter being the one equipped with the delay line (see Fig. 3d). This choice for the phase-matching angles is based on the fact that the four sequential reflections from the ML mirrors of the delay line *de facto* determine the photon frequency ( $\omega_3$ ) of the beam exiting the internal branch-line. The latter was chosen to be the third harmonic of the FEL radiation, a solution that hence gives the photon

frequency of the other two branch-lines ( $\omega_1 = \omega_2 = \omega_3/3$ ). Alternatively,  $\omega_1 = \omega_2$  and  $\omega_3$  can be the radiation coming from the first and second stage of the double-cascade seeded FEL source FEL-2 (Allaria *et al.*, 2013a). The ‘cuts’ in the transverse profile of the incoming beam made in order to derive the three FEL branch-lines and the transverse profiles of these three beams at the sample position are sketched in the insets of Fig. 3(d); such a situation is expected to maximize the effective spatial overlap of the three beams at the sample position, as also indicated by ray-tracing simulations [some of them are reported elsewhere (Cucini *et al.*, 2011a)]. In general, the focal spots created in the different configurations always present a greater horizontal size, ranging in the 200–500  $\mu\text{m}$  interval depending on the incidence angle on the sample, as compared with a more compressed vertical one (about 100  $\mu\text{m}$ ). Ideally each branch-line will be equipped with on-

line diagnostics to monitor the intensity and position of the three FEL beams impinging on the sample, since these parameters (as well as the intensity distribution of the FEL radiation in the interaction region) can affect the visibility of the transient gratings and hence the efficiency of the FWM process. At present such diagnostic devices are not installed; we are evaluating the use of intensity monitors based on the scattering from the residual gas in the vacuum pipes and four-quadrant photodiodes as beam position monitors. A study of the beam profiles in the various instrumental configurations is not planned but, most likely, will be carried out in the near future.

To date, the delay line of EIS-TIMER can host four sets of four ML mirrors (Naujok *et al.*, 2015), optimized to reflect photons at 69.3, 93.2, 185.1 and 391.2 eV while cutting the reflectivities at the corresponding first harmonic wavelengths of the FEL radiation (*i.e.* 23.1, 31.06, 61.7 and 130.4 eV). These four sets can be selected by a vertical translation of the translational stage of the delay line, while the crossing angle at the sample can be set at 18.4°, 27.6°, 79° and 105.4° by using four different sets of three toroidal mirrors, which can be selected by inserting/removing the toroidal mirrors in/from the pathways of the three beams. The combinations of such crossing angles and photon frequencies may allow the  $k$ -range between  $\sim 0.03$  and  $\sim 1 \text{ nm}^{-1}$  to be covered, which is the range of major interest for the study of vibrational dynamics in disordered systems and nanostructures. Furthermore, the extension of the photon frequency range of FERMI up to about 300 eV (achieved during the project development) would allow the  $k$ -range exploitable by TIMER to be extended up to about  $2.5 \text{ nm}^{-1}$ , a range nowadays met only by inelastic hard X-ray and thermal neutron scattering experiments. This will potentially make EIS-TIMER a powerful complementary time-resolved tool for such longstanding frequency resolved methods. In this context it is worth mentioning that time-domain measurements of X-ray diffuse scattering have been used to determine the phonon dispersion curves in a single-crystalline Ge sample, slightly photo-excited by an ultrafast optical pulse (Trigo *et al.*, 2013). Such a novel approach relies upon the measurements of the equal-time correlation function of density–density fluctuations as a function of the time delay between the optical (pump) and the X-ray (probe) pulses. An energy resolution of  $\sim 0.3 \text{ meV}$  (*i.e.* beyond that of most inelastic X-ray scattering spectrometers) and the possibility to reconstruct large portions of the single-crystalline dispersion relations in a single measure have been demonstrated (Zhu *et al.*, 2015).

We finally mention that the time delay between the two external branch-lines of EIS-TIMER can be varied in the  $-3/+7 \text{ ps}$  range by translating the toroidal mirrors of the branch-line 1, accompanied by a change in the pitch angle of PM2 and of the toroidal mirror, in order to keep the trajectory of the beam impinging into the sample fixed. This option was developed to finely adjust the time coincidence of the two equal-frequency FEL pulses, needed for ISS experiments, but can also be used to vary the delay between such pulses ( $\Delta t_{12}$ ) to carry out other kinds of FWM applications, such as, for

example, photon echo or two-dimensional spectroscopy. Moreover, when combined with the twin-seed two-color FEL operation mode of FERMI (Allaria *et al.*, 2013b), the control on  $\Delta t_{12}$  can be used to compensate for the time delay between the two-color FEL pulses, in order to bring into interaction two time-coincidence FEL pulses of different photon frequencies, which can be used for coherent Raman scattering studies (Bencivenga *et al.*, 2014).

With respect to the tentative layout proposed by some of us (Bencivenga & Masciovecchio, 2009), we dropped the use of diffractive optics to split the FEL beams. This choice is essentially motivated by the complexity in devising a system able to minimize the transverse and longitudinal chirp, as well as the lengthening of the FEL pulse duration, while maintaining an acceptable photon throughput and, most importantly, the option to exploit the full wavelength and polarization tunability provided by the FERMI FEL facility (Allaria *et al.*, 2012b, 2014). However, we are still considering the option of multi-gratings devices to split multi-color FEL pulses and to design an exceptionally compact optical setup for FEL-based FWM, which is briefly presented in the subsequent section.

The first commissioning activities on the EIS-TIMER beamline took place in the first week of July 2015; data are still under evaluation, we hereby report on the preliminary results. The main aim of the present commissioning period was to provide evidence for the generation of gratings due to the interference of the two FEL pulses coming from branch-lines 1 and 2. The beams were first aligned using reference targets along these two branch-lines and then focused at the sample position inside the experimental chamber. Figs. 4(a) and 4(b) show images of the beam profile on a fluorescent screen. The shape of the beam is an inclined ellipse of about  $50 \mu\text{m} \times 500 \mu\text{m}$  (a more accurate analysis of the beam dimension is ongoing), fairly larger than the expectations ( $\sim 50 \mu\text{m} \times 200 \mu\text{m}$ ). The larger dimensions of the focal spot in one plane and the inclined shape of the ellipse are likely ascribable to a misalignment of the toroidal mirrors. A more accurate optimization of the focus will be carried out in the near future. Once spatially overlapped we used a ‘jitter-free’ optical probe [the first harmonic of the Ti:sapphire seed-user laser available at FERMI (Danailov *et al.*, 2014)] to perform cross-correlation measurements based on FEL-induced transient optical reflectivity from a  $\text{Si}_3\text{N}_4$  reference sample (Casolari *et al.*, 2014). Measurements corresponding to the FEL beams coming from branch-line 1 and 2 are reported in Figs. 4(c) and 4(d). The relative time delay ( $\Delta t_{12} \simeq 1.7 \text{ ps}$ ) between the two FEL beams was successfully compensated by using the procedure devised for that purpose, *i.e.* a translation of  $\text{TM}_2$  along the nominal direction of the beam impinging into the chamber associated with the adjustment of the pitch angle of both  $\text{TM}_2$  and PM2 (see Fig. 3d). Cross-correlation measurements in such a condition are reported in Figs. 4(e) and 4(f). Once the temporal and spatial superposition of the two beams was ensured, we increased the FEL fluence in order to exploit the radiation damage for printing permanent gratings into a  $\text{SiO}_2$  sample. Atomic force microscopy (AFM) measurements

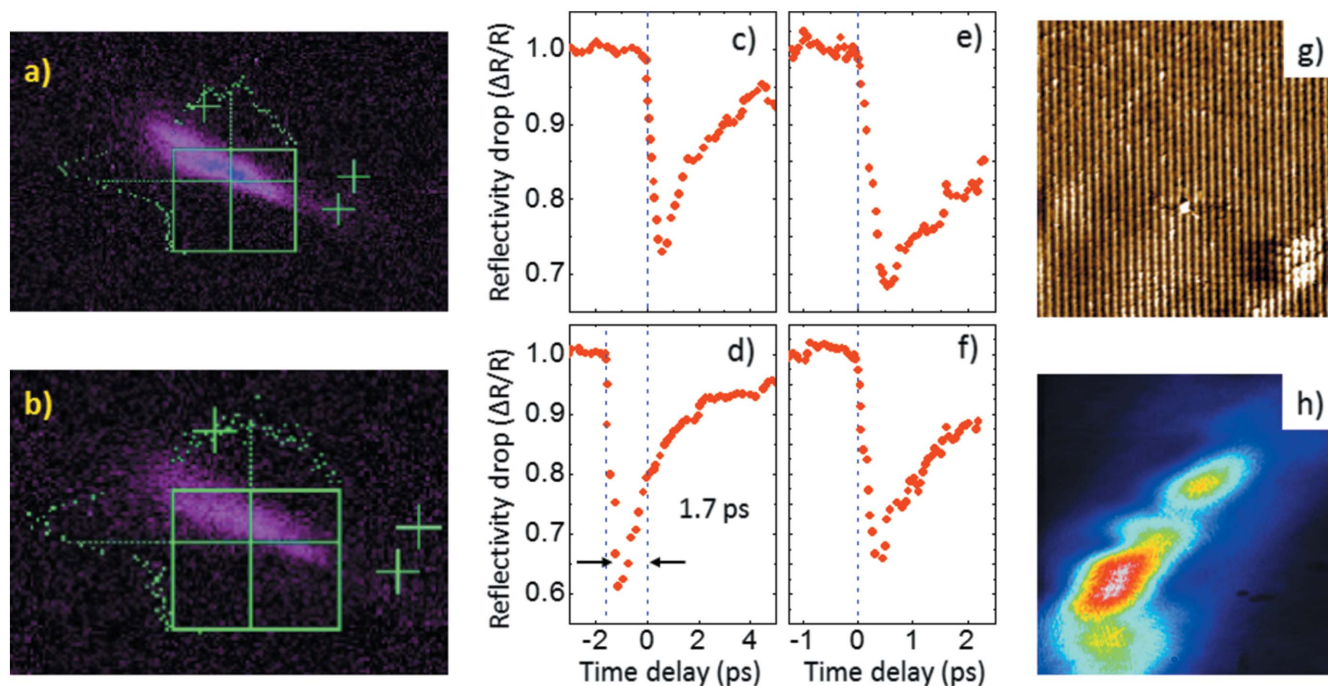


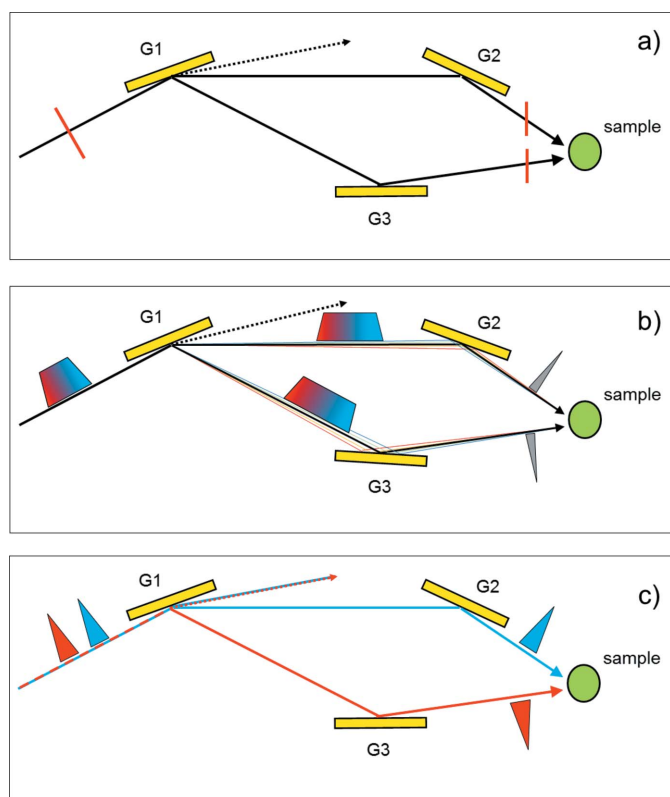
**Figure 4** Images of the FEL beams coming from the branch-line 1 (a) and 2 (b) on a fluorescent screen. Cross-correlations measurements corresponding to the beam from branch-line 1 (c) and 2 (d). (e) and (f) are as (c) and (d), respectively, after the equalization of the relative time delay between the two FEL beams. (g) AFM topography of the permanent grating generated by the interference between the two FEL beams where the printed grating can be clearly seen. (h) CCD image of the UV laser beam diffracted by a FEL-generated grating.

on the damaged sample bear clear evidence of the successful generation of such gratings, characterized by a pitch  $L = 150 \text{ nm} \pm 15 \text{ nm}$  [ $L = \lambda_{\text{FEL}}/2\sin(\theta)$ ] fully compatible with the employed experimental geometry (crossing angle  $2\theta \simeq 18.4^\circ$ ) and FEL wavelength ( $\lambda_{\text{FEL}} = 51.2 \text{ nm}$ ); an AFM topography is shown in Fig. 4(g). This result unambiguously demonstrates the occurrence of interference between the two EUV light fields, essential prerequisite for FEL-based FWM experiments. The grating patterns do not extend for the entire damaged region, since the effective dimension of the interaction region in the horizontal plane is limited to  $\sim c\delta t/\tan(2\theta) \simeq 100 \mu\text{m}$  (where  $c$  is the speed of light and  $\delta t \simeq 100 \text{ fs}$  is the FEL pulse duration) by the tilted wavefronts of the interfering FEL beams. AFM measurements on gratings printed at different space–time overlap conditions are ongoing. We finally used a UV laser beam (*i.e.* the third harmonic of the Ti:sapphire seed-user laser:  $\lambda_{\text{laser}} \simeq 262 \text{ nm}$ ) and a system, integrated into the experimental end-station, able to roto-translate the laser beam keeping the pivot at the sample position fixed to observe the diffracted signal from the FEL-generated gratings. Fig. 4(h) shows a CCD image of the UV laser beam diffracted by the grating; the irregular shape of the diffraction spot may indicate an irregular intensity distribution of the beams in the interaction region. This aspect is likely related to the non-optimized FEL focusing and will be investigated in the forthcoming commissioning shifts. The lack of time prevented us from looking for a transient grating signal; however, the occurrence of the interference between the crossed FEL beams and the capability to observe it with an external laser are in principle the only requirements for

observing ISS signals stimulated by EUV/soft X-ray transient gratings.

### 2.3. nano-TIMER

As quoted before, we are evaluating the possibility to realise a third experimental setup based on diffractive optics (nano-TIMER; see Fig. 5), purposely designed for specific FEL-based FWM experiments, even more compact than mini-TIMER. The potential advantages in using diffractive optics are multiple. First of all it is possible to design a compact system that can be hosted inside an already existing experimental chamber. Moreover, by playing with the grating parameters (angle of incidence, diffraction orders, grating pitch, blazing angles, *etc.*) it is in principle possible: (i) tilt the wavefronts of the interfering beams (see Fig. 5a) in order to optimize the overlap between the two pulses when recombined (David *et al.*, 2015); (ii) compress the FEL pulses, if chirped at the source, reaching pulse durations down to the femtosecond scale (see Fig. 5b), and (iii) separate in angle multi-color collinear FEL pulses (see Fig. 5c). The latter feature is of great interest for more advanced FWM applications, that have been recently proposed (Bencivenga *et al.*, 2014) after the demonstration of the two-color seeded FEL emission (Allaria *et al.*, 2013b). In more detail the system is expected to be composed of a plane diffraction grating (G1), located downstream from a focusing mirror, devoted to angularly separate the incoming photon beams (same color or multi-colors) and stretch the pulses in time. After a short path the beams impinge over two different diffraction gratings (G2


**Figure 5**

Sketch of a splitting-and-recombination setup based on diffractive gratings (G1, G2 and G3). In principle the use of gratings instead of diffractive optics would allow to control the wavefront tilt at the sample [sketched by the red segments in (a)], compress in time chirped FEL pulses (b) and split two-colors FEL pulses (c).

and G3, one for each pulse) and are diffracted again over the sample being compressed and tilted. In this way the outgoing photon beams have been separated, compressed, tilted and recombined over the sample. All this may allow FWM experiments to be extended to an unprecedented dynamic range (multi-color option) and time resolution (compression), with the benefit of the improved superposition (wavefront tilt). Apart from the difficulty of designing and realising such a complicated system, the main drawbacks lie in the total transmission of the diffractive optics, which will be much lower compared with the mini-TIMER and EIS-TIMER solutions where only grazing-incidence mirrors are employed, and in the need to use different gratings for specific FEL parameters (photon frequency, time duration, photon frequency difference in multi-color mode, *etc.*) and crossing angles. In our calculations and according to recent tests (October 2015) on the fluence dependence of the FWM signal carried out on mini-Timer (Bencivenga, unpublished), the fluence at the sample is expected to be high enough to create and detect the signal from the recombined FEL pulses. A more general solution employing also the third harmonic of the FEL emission as a probe pulse is under investigation. The whole system as well as the expected performances and possible experiments will be soon described in a dedicated publication.

### 3. Conclusions

The success of our tests on mini-TIMER, which is already available at FERMI for user experiments, and on EIS-TIMER, which has just started its commissioning activities, opens up the entire new field of non-linear optics at sub-optical wavelengths with access to a broad range of excitations and will also provide the element specificity exploiting core level excitations. This would enable, for example, charge and energy flows between constituent atoms in materials to be followed, capabilities not attainable using table-top lasers and/or synchrotrons. Within the several fundamental scientific issues that can be addressed by the use of EUV/soft X-ray FWM we may mention: intramolecular relaxation dynamics in metal complexes, dynamics of charge injection, transport and photocatalytic reactions in metal oxides nanoparticles, dynamics of porphyrins that are involved in important biological processes (oxygen transport, photosynthesis) and play an important role in light-energy conversion, molecular sensing, spintronics, data storage and magnetic switching.

### Acknowledgements

M. Svandrlik and all the FERMI team are gratefully acknowledged for their valuable support. The authors acknowledge support from the European Research Council through the ERC Grant N.202804-TIMER.

### References

- Allaria, E., Appio, R., Badano, L., Barletta, W. A., Bassanese, S., Biedron, S. G., Borga, A., Busetto, E., Castronovo, D., Cinquegrana, P., Cleva, S., Cocco, D., Cornacchia, M., Craievich, P., Cudin, I., D'Auria, G., Dal Forno, M., Danailov, M. B., De Monte, R., De Ninno, G., Delgiusto, P., Demidovich, A., Di Mitri, S., Diviacco, B., Fabris, A., Fabris, R., Fawley, W., Ferianis, M., Ferrari, E., Ferry, S., Froehlich, L., Furlan, P., Gaio, G., Gelmetti, F., Giannessi, L., Giannini, M., Gobessi, R., Ivanov, R., Karantzoulis, E., Lonza, M., Lutman, A., Mahieu, B., Molloch, M., Milton, S. V., Musardo, M., Nikolov, I., Noe, S., Parmigiani, F., Penco, G., Petronio, M., Pivetta, L., Predonzani, M., Rossi, F., Rumiz, L., Salom, A., Scafuri, C., Serpico, C., Sigalotti, P., Spampinati, S., Spezzani, C., Svandrlik, M., Svetina, C., Tazzari, S., Trovo, M., Umer, R., Vascotto, A., Veronese, M., Visintini, R., Zaccaria, M., Zangrando, D. & Zangrando, M. (2012a). *Nat. Photon.* **6**, 699–704.
- Allaria, E., Battistoni, A., Bencivenga, F., Borghes, R., Callegari, C., Capotondi, F., Castronovo, D., Cinquegrana, P., Cocco, D., Coreno, M., Craievich, P., Cucini, R., D'Amico, F., Danailov, M. B., Demidovich, A., De Ninno, G., Di Cicco, A., Di Fonzo, S., Di Fraia, M., Di Mitri, S., Diviacco, B., Fawley, W. M., Ferrari, E., Filipponi, A., Froehlich, L., Gessini, A., Giangrisostomi, E., Giannessi, L., Giuressi, D., Grazioli, C., Gunnella, R., Ivanov, R., Mahieu, B., Mahne, N., Masciovecchio, C., Nikolov, I. P., Passos, G., Pedersoli, E., Penco, G., Principi, E., Raimondi, L., Sergo, R., Sigalotti, P., Spezzani, C., Svetina, C., Trovò, M. & Zangrando, M. (2012b). *New J. Phys.* **14**, 113009.
- Allaria, E., Bencivenga, F., Borghes, R., Capotondi, F., Castronovo, D., Charalambous, P., Cinquegrana, P., Danailov, M. B., De Ninno, G., Demidovich, A., Di Mitri, S., Diviacco, B., Fausti, D., Fawley, W. M., Ferrari, E., Froehlich, L., Gauthier, D., Gessini, A., Giannessi, L., Ivanov, R., Kiskinova, M., Kurdi, G., Mahieu, B., Mahne, N., Nikolov, I., Masciovecchio, C., Pedersoli, E., Penco, G., Raimondi, L., Serpico, C., Sigalotti, P., Spampinati, S., Spezzani, C.,

- Svetina, C., Trovò, M. & Zangrando, M. (2013b). *Nat. Commun.* **4**, 2476.
- Allaria, E., Castronovo, D., Cinquegrana, P., Craievich, P., Dal Forno, M., Danailov, M. B., D'Auria, G., Demidovich, A., De Ninno, G., Di Mitri, S., Diviacco, B., Fawley, W. M., Ferianis, M., Ferrari, E., Froehlich, L., Gaio, G., Gauthier, D., Giannessi, L., Ivanov, R., Mahieu, B., Mahne, N., Nikolov, I., Parmigiani, F., Penco, G., Raimondi, L., Scafuri, C., Serpico, C., Sigalotti, P., Spampinati, S., Spezzani, C., Svandrlik, M., Svetina, C., Trovo, M., Veronese, M., Zangrando, D. & Zangrando, M. (2013a). *Nat. Photon.* **7**, 913–918.
- Allaria, E., Diviacco, B., Callegari, C., Finetti, P., Mahieu, B., Viehhaus, J., Zangrando, M., De Ninno, G., Lambert, G., Ferrari, E., Buck, J., Ichen, M., Vodungbo, B., Mahne, N., Svetina, C., Spezzani, C., Di Mitri, S., Penco, G., Trovò, M., Fawley, W. M., Rebernik, P. R., Gauthier, D., Grazioli, C., Coreno, M., Ressel, B., Kivimäki, A., Mazza, T., Glaser, L., Scholz, F., Seltmann, J., Gessler, P., Grünert, J., De Fanis, A., Meyer, M., Knie, A., Moeller, S. P., Raimondi, L., Capotondi, F., Pedersoli, E., Plekan, O., Danailov, M. B., Demidovich, A., Nikolov, I., Abrami, A., Gautier, J., Lüning, J., Zeitoun, P. & Giannessi, L. (2014). *Phys. Rev. X*, **4**, 041040.
- Bencivenga, F., Baroni, S., Carbone, C., Chergui, M., Danailov, M. B., De Ninno, G., Kiskinova, M., Raimondi, L., Svetina, C. & Masciovecchio, C. (2013). *New J. Phys.* **15**, 123023.
- Bencivenga, F., Capotondi, F., Casolari, F., Dallari, F., Danailov, M. B., De Ninno, G., Fausti, D., Kiskinova, M., Manfreda, M., Masciovecchio, C. & Pedersoli, E. (2014). *Faraday Discuss.* **171**, 487–503.
- Bencivenga, F., Cucini, R., Capotondi, F., *et al.* (2015b). *Proc. SPIE*, **9512**, 951212.
- Bencivenga, F., Cucini, R., Capotondi, F., Battistoni, A., Mincigrucchi, R., Giangrisostomi, E., Gessini, A., Manfreda, M., Nikolov, I. P., Pedersoli, E., Principi, E., Svetina, C., Parrisè, P., Casolari, F., Danailov, M. B., Kiskinova, M. & Masciovecchio, C. (2015a). *Nature (London)*, **520**, 205–208.
- Bencivenga, F. & Masciovecchio, C. (2009). *Nucl. Instrum. Methods Phys. Res. A*, **606**, 785–789.
- Beye, M., Schreck, S., Sorgenfrei, F., Trabant, C., Pontius, N., Schüssler-Langeheine, C., Wurth, W. & Föhlisch, A. (2013). *Nature (London)*, **501**, 191–194.
- Bloembergen, N. (1982). *Rev. Mod. Phys.* **54**, 685–695.
- Boyd, R. (2008). *Nonlinear Optics*. New York: Academic Press.
- Cameron, A. R., Riblet, P. & Miller, A. (1996). *Phys. Rev. Lett.* **76**, 4793–4796.
- Capotondi, F., Pedersoli, E., Bencivenga, F., Manfreda, M., Mahne, N., Raimondi, L., Svetina, C., Zangrando, M., Demidovich, A., Nikolov, I., Danailov, M., Masciovecchio, C. & Kiskinova, M. (2015). *J. Synchrotron Rad.* **22**, 544–552.
- Capotondi, F., Pedersoli, E., Mahne, N., Menk, R. H., Passos, G., Raimondi, L., Svetina, C., Sandrin, G., Zangrando, M., Kiskinova, M., Bajt, S., Barthelmess, M., Fleckenstein, H., Chapman, H. N., Schulz, J., Bach, J., Frömter, R., Schleitzer, S., Müller, L., Gutt, C. & Grübel, G. (2013). *Rev. Sci. Instrum.* **84**, 051301.
- Casolari, F., Bencivenga, F., Capotondi, F., Giangrisostomi, E., Manfreda, M., Mincigrucchi, R., Pedersoli, E., Principi, E., Masciovecchio, C. & Kiskinova, M. (2014). *Appl. Phys. Lett.* **104**, 191104.
- Cucini, R., Battistoni, A., Gessini, A., Bencivenga, F., Principi, E., Saito, M., D'Amico, F., Sergo, R. & Masciovecchio, C. (2014). *Opt. Lett.* **39**, 5110–5113.
- Cucini, R., Bencivenga, F. & Masciovecchio, C. (2011a). *Opt. Lett.* **36**, 1032–1034.
- Cucini, R., Bencivenga, F., Zangrando, M. & Masciovecchio, C. (2011b). *Nucl. Instrum. Methods Phys. Res. A*, **635**, S69–S74.
- Danailov, M. B., Bencivenga, F., Capotondi, F., Casolari, F., Cinquegrana, P., Demidovich, A., Giangrisostomi, E., Kiskinova, M. P., Kurdi, G., Manfreda, M., Masciovecchio, C., Mincigrucchi, R., Nikolov, I. P., Pedersoli, E., Principi, E. & Sigalotti, P. (2014). *Opt. Express*, **22**, 12869–12879.
- David, C., Karvinen, P., Sikorski, M., Song, S., Vartiainen, I., Milne, C. J., Mozzanica, A., Kayser, Y., Diaz, A., Mohacsi, I., Carini, G. A., Herrmann, S., Färm, E., Ritala, M., Fritz, D. M. & Robert, A. (2015). *Sci. Rep.* **5**, 7644.
- Dhar, L., Rogers, J. A. & Nelson, K. A. (1994). *Chem. Rev.* **94**, 157–193.
- Ferrante, C., Pontecorvo, E., Cerullo, G., Chiasera, A., Ruocco, G., Schirmacher, W. & Scopigno, T. (2013). *Nat. Commun.* **4**, 1793.
- Glover, T. E., Fritz, D. M., Cammarata, M., Allison, T. K., Coh, S., Feldkamp, J. M., Lemke, H., Zhu, D., Feng, Y., Coffee, R. N., Fuchs, M., Ghimire, S., Chen, J., Shwartz, S., Reis, D. A., Harris, S. E. & Hastings, J. B. (2012). *Nature (London)*, **488**, 603–608.
- Lewis, A. & Lieberman, K. (1991). *Nature (London)*, **354**, 214–216.
- Li, X., Voss, P. L., Sharping, J. E. & Kumar, P. (2005). *Phys. Rev. Lett.* **94**, 053601.
- Masciovecchio, C., Battistoni, A., Giangrisostomi, E., Bencivenga, F., Principi, E., Mincigrucchi, R., Cucini, R., Gessini, A., D'Amico, F., Borghes, R., Prica, M., Chenda, V., Scarcia, M., Gaio, G., Kurdi, G., Demidovich, A., Danailov, M. B., Di Cicco, A., Filipponi, A., Gunnella, R., Hatada, K., Mahne, N., Raimondi, L., Svetina, C., Godnig, R., Abrami, A. & Zangrando, M. (2015). *J. Synchrotron Rad.* **22**, 553–564.
- Naujok, P., Yulin, S., Bianco, A., Mahne, N., Kaiser, N. & Tünnermann, A. (2015). *Opt. Express*, **23**, 4289–4295.
- Nelson, K. A., Miller, R. J. D., Lutz, D. R. & Fayer, M. D. (1982). *J. Appl. Phys.* **53**, 1144–1149.
- Patterson, B. D. (2010). SLAC Technical Note SLAC-TN-10-026. SLAC, Stanford, CA, USA.
- Raimondi, L., Svetina, C., Mahne, N., Cocco, D., Abrami, A., De Marco, M., Fava, C., Gerusina, S., Gobessi, R., Capotondi, F., Pedersoli, E., Kiskinova, M., De Ninno, G., Zeitoun, P., Dovillaire, G., Lambert, G., Boutu, W., Merdji, H., Gonzalez, A. I., Gauthier, D. & Zangrando, M. (2013). *Nucl. Instrum. Methods Phys. Res. A*, **710**, 131–138.
- Rohringer, N., Ryan, D., London, R. A., Purvis, M., Albert, F., Dunn, J., Bozek, J. D., Bostedt, C., Graf, A., Hill, R., Hau-Riege, S. P. & Rocca, J. J. (2012). *Nature (London)*, **481**, 488–491.
- Shvyd'ko, Y., Stoupin, S., Shu, D., Collins, S. P., Mundboth, K., Sutter, J. & Tolkiehn, M. (2014). *Nat. Commun.* **5**, 4219.
- Shwartz, S., Fuchs, M., Hastings, J. B., Inubushi, Y., Ishikawa, T., Katayama, T., Reis, D. A., Sato, T., Tono, K., Yabashi, M., Yudovich, S. & Harris, S. E. (2014). *Phys. Rev. Lett.* **112**, 163901.
- Tamasaku, K., Shigemasa, E., Inubushi, Y., Katayama, T., Sawada, K., Yumoto, H., Ohashi, H., Mimura, H., Yabashi, M., Yamauchi, K. & Ishikawa, T. (2014). *Nat. Photon.* **8**, 313–316.
- Tanaka, S. & Mukamel, S. (2002). *Phys. Rev. Lett.* **89**, 043001.
- Trigo, M., Fuchs, M., Chen, J., Jiang, M. P., Cammarata, M., Fahy, S., Fritz, D. M., Gaffney, K., Ghimire, S., Higginbotham, A., Johnson, S. L., Kozina, M. E., Larsson, J., Lemke, H., Lindenberg, A. M., Ndabashimiye, G., Quirin, F., Sokolowski-Tinten, K., Uher, C., Wang, G., Wark, J. S., Zhu, D. & Reis, D. A. (2013). *Nat. Phys.* **9**, 790–794.
- Zangrando, M., Abrami, A., Bacescu, D., Cudin, I., Fava, C., Frassetto, F., Galimberti, A., Godnig, R., Giuressi, D., Poletto, L., Rumiz, L., Sergo, R., Svetina, C. & Cocco, D. (2009). *Rev. Sci. Instrum.* **80**, 113110.
- Zangrando, M., Cocco, D., Fava, C., Gerusina, S., Gobessi, R., Mahne, N., Mazzucco, E., Raimondi, L., Rumiz, L. & Svetina, C. (2015). *J. Synchrotron Rad.* **22**, 565–570.
- Zhu, D., Robert, A., Henighan, T., Lemke, H. T., Chollet, M., Glowacki, J. M., Reis, D. A. & Trigo, M. (2015). *Phys. Rev. B*, **92**, 054303.